

Spectroelectrochemistry of metalloporphyrins

Karl M. Kadish and Xihai Mu

Department of Chemistry, University of Houston,
Houston, Texas 77204-5641, U.S.A.

Abstract - Three examples have been selected to illustrate the application and benefits of thin-layer spectroelectrochemistry for monitoring metalloporphyrin redox reactions. These examples show how FTIR, UV-visible and ESR spectroelectrochemical techniques can be combined to monitor the site of oxidation/reduction, the fate of the bound diatomic molecule after electron transfer, the type of π cation radical generated and the spectral properties of a product formed in reactions between an electroreduced porphyrin and the methylene chloride solvent.

INTRODUCTION

Metalloporphyrins with over four dozen different central metals have been electrochemically characterized (ref. 1). These reactions may occur at the central metal ion, at the porphyrin π ring system, or at the coordinated axial ligand. The site of electron transfer can sometimes be suggested by trends in half-wave potentials, but a definite assignment can only come from evaluation of spectral data for the oxidized and/or reduced species on time scales approaching those of the electrochemical measurement. The optimum way to accomplish this is via thin-layer spectroelectrochemistry.

Three examples from the literature have been selected to illustrate the application and benefits of thin-layer spectroelectrochemistry for monitoring metalloporphyrin redox reactions. These are: (1) the reduction of (P)Ru(CO) in tetrahydrofuran (where P = the dianion of tetraphenylporphyrin (TPP) or octaethylporphyrin (OEP)), (2) the oxidation of (OEP)Ir(CO)Cl in methylene chloride and, (3) the oxidation and reduction of (TPP)Co(NO) in methylene chloride.

EXPERIMENTAL

Construction of UV-visible (ref. 2), FTIR (ref. 3,4), and ESR (ref. 5) thin-layer spectroelectrochemical cells and associated electrochemical/spectroscopic instrumentation are described in the literature. Microelectrode voltammetry was carried out as described in ref. 4. (TPP)Ru(CO) (ref. 6), (OEP)Ru(CO) (ref. 7), (OEP)Ir(CO)Cl (ref. 8) and (TPP)Co(NO) (ref. 9) were synthesized by literature methods. Tetrahydrofuran, methylene chloride and tetrabutylammonium perchlorate were purified using standard methods.

RESULTS AND DISCUSSION

FTIR and UV-visible monitoring of (P)Ru(CO) reduction

(TPP)Ru(CO) and (OEP)Ru(CO) are reduced in two reversible one electron transfer steps as illustrated in Figure 1. Overall, four possible products may result from the first reduction. These are given by reactions 1-4 shown in Scheme I. Previous studies of (P)Ru(CO) (ref. 10,11) suggest that the first electron is reversibly added to the porphyrin π ring system but no spectroscopic evidence was presented to confirm this.

FTIR spectra before and after electroreduction of (P)Ru(CO) are given in Figures 2a and 2b. The TPP complex has a CO vibration at 1941 cm^{-1} (Fig. 2a) before reduction while the vibration of the OEP complex (Fig. 2b) is at 1931 cm^{-1} . Both vibrations appear as negative peaks in the difference FTIR spectra as (P)Ru(CO) is consumed (ref. 4). Positive peaks at 1898 cm^{-1} (TPP) and 1894 cm^{-1} (OEP) are attributed to the CO vibration of singly reduced [(P)Ru(CO)]⁻. These data indicate that CO remains coordinated after electroreduction and the shift of the CO vibration to lower frequencies is consistent with an increased negative charge on the metal center. On the basis of these data, reactions 3 and 4 in Scheme I can be eliminated as possible electroreduction mechanisms of (P)Ru(CO).

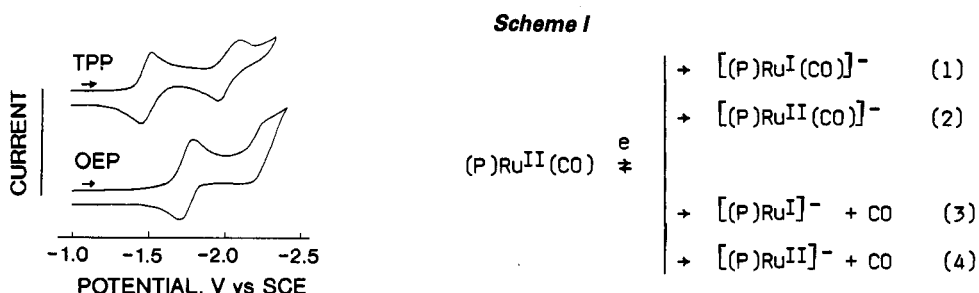


Fig. 1. Cyclic voltammograms and possible reactions of $(P)Ru(CO)$ at a $25 \mu m$ Pt micro-electrode in tetrahydrofuran containing $0.1 M$ tetrabutylammonium perchlorate. Scan rate = $10 V s^{-1}$.

UV-visible spectra generated during the first reduction of $(TPP)Ru(CO)$ and $(OEP)Ru(CO)$ are shown in Figures 2c and 2d. The two complexes give quite different types of spectral changes. Electrogenerated $[(TPP)Ru(CO)]^-$ has a much decreased Soret band intensity and is consistent with the formation of a porphyrin π anion radical (rxn. 2). On the other hand, the spectral changes for $(OEP)Ru(CO)$ are similar to those for reduction of $(TPP)Ag^{II}$ to give $[(TPP)Ag^I]^-$ (ref. 12) and, on this basis, a metal centered reduction (rxn 1) is postulated to occur for $(OEP)Ru(CO)$. Thus, the similar electrochemistry of the two $(P)Ru(CO)$ complexes gives no indication of different electron transfer mechanisms which are only shown by the UV-visible spectroelectrochemistry.

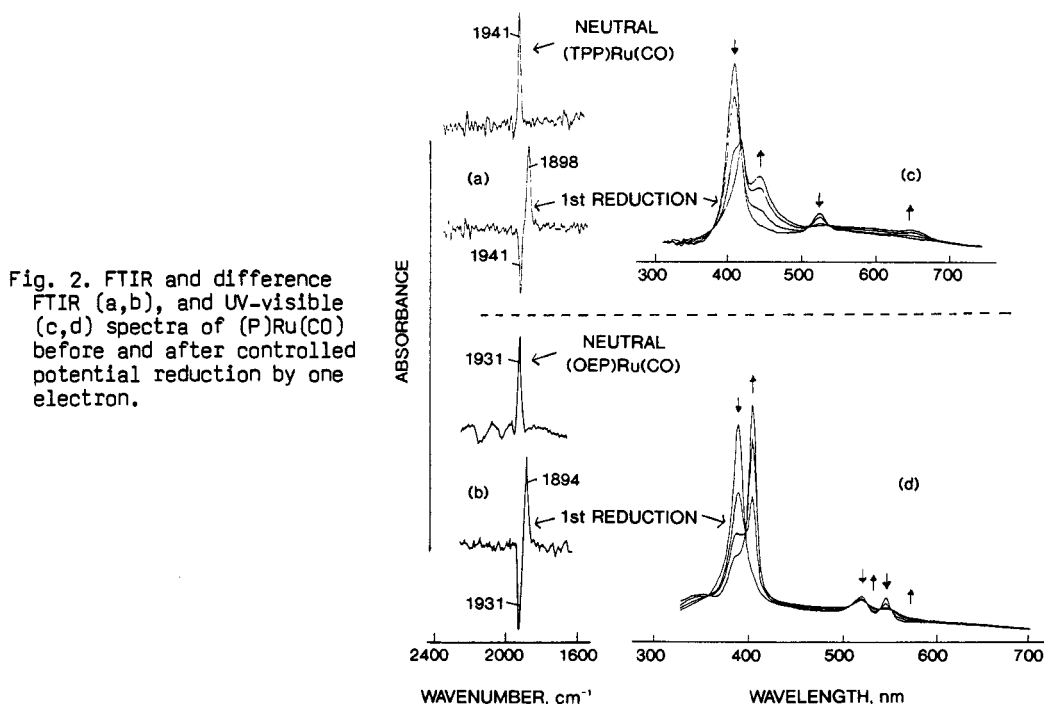
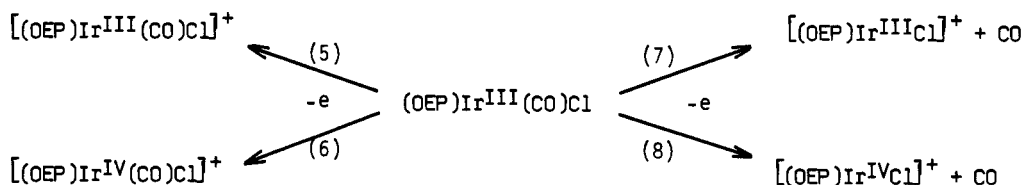


Fig. 2. FTIR and difference FTIR (a,b), and UV-visible (c,d) spectra of $(P)Ru(CO)$ before and after controlled potential reduction by one electron.

FTIR and ESR monitoring of $(OEP)Ir(CO)Cl$ oxidation

$(OEP)Ir(CO)Cl$ can be oxidized in two reversible steps (ref. 8). The first step may generate either an $Ir(III)$ or an $Ir(IV)$ porphyrin which may or may not be complexed with CO as shown by the four electrode reactions given in Scheme II:

Scheme II



A cyclic voltammogram of $(\text{OEP})\text{Ir}(\text{CO})\text{Cl}$ is illustrated in Figure 3a while the FTIR spectrum of the complex is shown in Figure 3b. The initial porphyrin has a CO vibration at 2056 cm^{-1} which may be compared to 2081 cm^{-1} for the singly oxidized complex (Figure 3c). There is also a well defined π cation radical marker band (ref. 13) at 1539 cm^{-1} . These two pieces of combined data are self consistent only with reaction 5 in Scheme II.

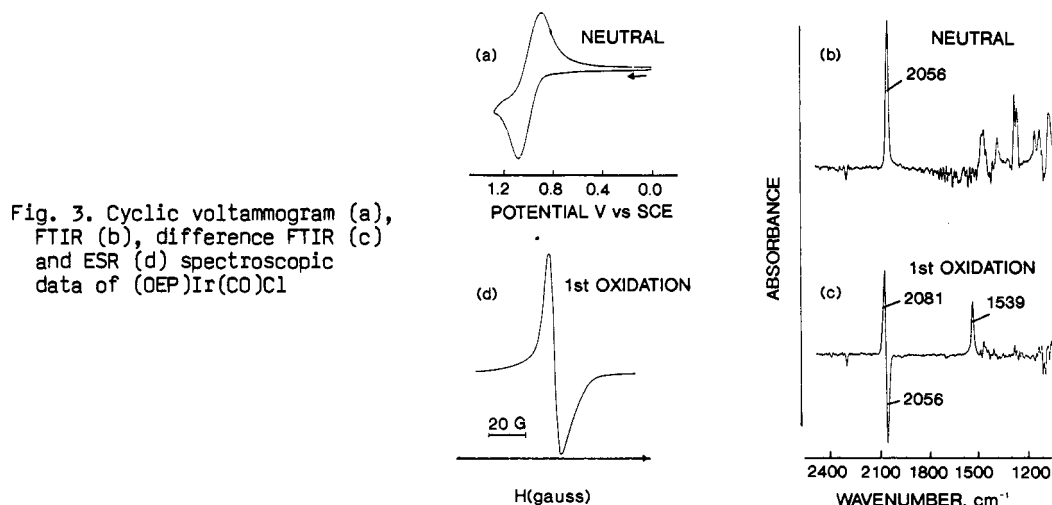


Fig. 3. Cyclic voltammogram (a), FTIR (b), difference FTIR (c) and ESR (d) spectroscopic data of $(\text{OEP})\text{Ir}(\text{CO})\text{Cl}$

Confirmation of reaction 5 as the prevailing mechanism also comes from the ESR spectrum in Fig. 3d. The ESR spectrum of $[(\text{OEP})\text{Ir}(\text{CO})\text{Cl}]^+$ has a $g = 2.00$ and a $\Delta H = 5.6\text{ G}$. The combination of ESR and FTIR spectroelectrochemical data in Fig. 3b-d clearly demonstrate the site of electron transfer and the fate of coordinated CO after oxidation. Information of this type cannot be obtained from a voltammogram of the type shown in Fig. 3a.

FTIR, UV-visible and ESR monitoring of $(\text{TPP})\text{Co}(\text{NO})$ oxidation/reduction

A cyclic voltammogram of $(\text{TPP})\text{Co}(\text{NO})$ in methylene chloride at a $25\text{ }\mu\text{m}$ microelectrode is shown in Figure 4 (ref. 14). The site of the first oxidation/reduction may occur at the Co(II) center or at the porphyrin π ring system as shown by the four electron transfer reactions given in Scheme III:

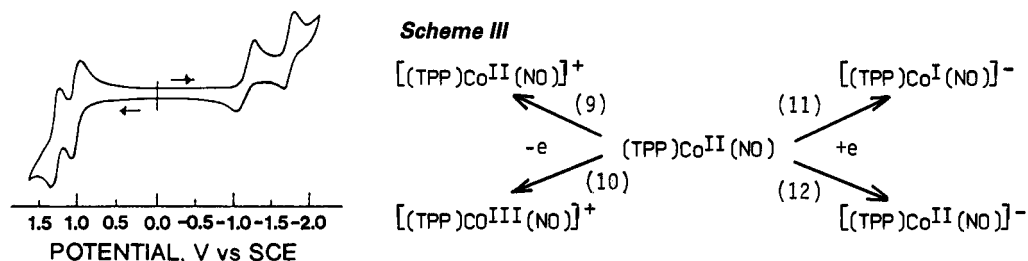


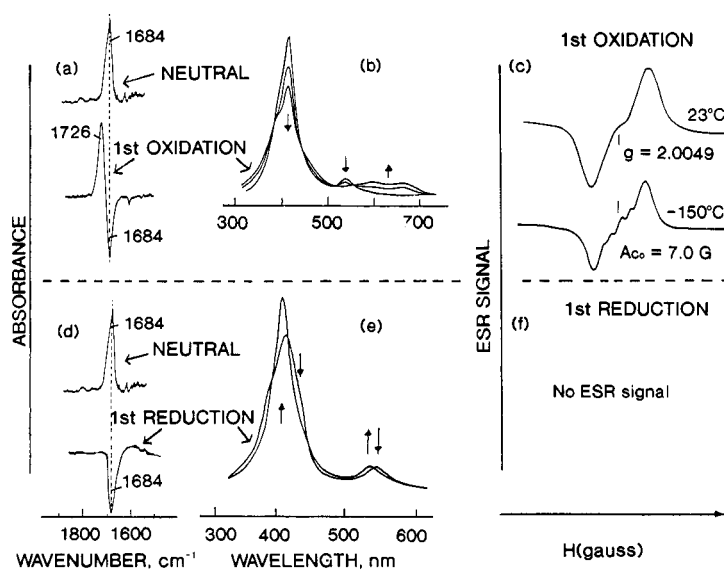
Fig. 4. Cyclic voltammogram and possible electron transfer reactions of $(\text{TPP})\text{Co}(\text{NO})$ at a $25\text{ }\mu\text{m}$ microelectrode in CH_2Cl_2 . Scan rate = 10 V s^{-1} .

Spectra obtained during the first oxidation confirm the formation of $[(\text{TPP})\text{CoIII}(\text{NO})]^+$. The FTIR spectrum of $[(\text{TPP})\text{CoIII}(\text{NO})]^+$ has a vibration at 1726 cm^{-1} (see Fig. 5a) and is consistent with a coordinated NO group. Both the UV-visible (Fig. 5b) and the ESR (Fig. 5c) spectra of $[(\text{TPP})\text{CoIII}(\text{NO})]^+$ are typical of a porphyrin π cation radical (ref. 15). There is a well-resolved splitting from Co(II) and the coupling constant of 7.0 G indicates a strong interaction between the unpaired electron on the $[(\text{TPP})\text{CoIII}(\text{NO})]^+$ porphyrin ring and the cobalt nuclei (ref. 15,16). This is consistent with an A_{2U} rather than an A_{1U} type radical (ref. 16)

The FTIR data for singly reduced $(\text{TPP})\text{Co}(\text{NO})$ (Fig. 5d) indicate a loss of NO after reduction by one electron while the UV-visible and ESR data (Fig. 5e,f) are consistent with the occurrence of a homogenous chemical reaction to generate an ESR silent species. The UV-visible spectrum of the final product in Figure 5e is identical to that of

(TPP)Co(CH₂Cl) (ref. 17) and the most probable reaction involves [(TPP)Co]⁻ (generated from [(TPP)Co^I(NO)]⁻ upon NO loss) and methylene chloride to give the σ-bonded complex.

Fig. 5. FTIR, difference FTIR, UV-visible and ESR monitoring of the products formed during oxidation (a-c) and reduction (d-f) of (TPP)Co(NO) in CH₂Cl₂



SUMMARY

This paper has presented three examples of in-situ spectroscopic data which are obtained during the oxidation and/or reduction of metalloporphyrins containing coordinated CO or NO axial ligands. The first example demonstrates how thin-layer FTIR and UV-visible spectroscopy can be combined to evaluate the site of electroreduction and the fate of the bound CO group after reduction of the complex by one electron. The second example shows how FTIR and ESR spectroelectrochemistry can be combined to evaluate the site of electrooxidation and the fate of the bound CO group after oxidation of the complex by one electron. The final example demonstrates how all three spectroelectrochemical techniques can be combined to monitor the site of oxidation/reduction, the fate of the bound NO group after electron transfer, the type of π cation radical generated and the spectral properties of a product formed in reactions between an electrogenerated Co(I) porphyrin and methylene chloride. The key point that must be emphasized is that oxidation/reduction potentials are not sufficient to determine the products of these electron transfer reactions and that more than one type of spectral characterization must be utilized.

REFERENCES

1. K.M. Kadish, *Prog. Inorg. Chem.* **34**, 435 (1986).
2. X.Q. Lin and K.M. Kadish, *Anal. Chem.* **57**, 1498 (1985).
3. K.M. Kadish, X.H. Mu and X.Q. Lin, *Electroanalysis* **1**, 35 (1989).
4. X.H. Mu and K.M. Kadish, *Inorg. Chem.* **27**, 4720 (1988).
5. X.H. Mu and K.M. Kadish, *Electroanalysis*, submitted for publication.
6. A. Adler, F. Longo, J. Finarelli, J. Goldmacher, J. Assour and L. Kaasakoff, *J. Org. Chem.* **32**, 476 (1967).
7. H.W. Whitlock and R. Hanauer, *J. Org. Chem.* **33**, 2169 (1968).
8. C. Swistak, J.-L. Cornillon, J.E. Anderson and K.M. Kadish., *Organometallics* **6**, 2146 (1987).
9. W.R. Scheidt and J.L. Hoard, *J. Am. Chem. Soc.* **95**, 8281 (1973).
10. K.M. Kadish and D. Chang, *Inorg. Chem.* **21**, 3614 (1982).
11. D.P. Rillema, J.K. Nagel, L.F. Berringer, Jr. and T.J. Meyer, *J. Am. Chem. Soc.* **103**, 56 (1981).
12. K.M. Kadish, X.Q. Lin, J.Q. Ding, Y.T. Wu and C. Araullo, *Inorg. Chem.* **25**, 3236 (1986).
13. E.T. Shimonura, M.A. Phillippi, H.M. Goff, W.F. Scholz and C.A. Reed, *J. Am. Chem. Soc.* **103**, 6778 (1981).
14. K.M. Kadish, X.H. Mu and X.Q. Lin, *Inorg. Chem.* **27**, 1489 (1988).
15. E. Fujita, C.K. Chang, J. Faier, *J. Am. Chem. Soc.* **107**, 7665 (1988).
16. K. Ichimol, H. Ohya-Nishiguchi, N. Hirota, and K. Yamamoto, *Bull Chem. Soc. Jpn.* **58**, 623 (1985).
17. K.M. Kadish, X.Q. Lin, and B.C. Han, *Inorg. Chem.* **26**, 4161 (1987).